Wideband Circularly Polarized Tightly Coupled Array

Long Zhang, Steven Gao, Senior Member, IEEE, Qi Luo, Member, IEEE, Wenting Li, Yejun He, Senior Member, IEEE, and Qingxia Li, Member, IEEE

Abstract—**Tightly coupled arrays (TCA) have received considerable interests recently. Although various TCAs have been reported, they are limited to single or dual linear polarizations. Considering the importance of circular polarization (CP) in various wireless systems, it is meaningful to design a CP TCA with a simple configuration. This paper presents a circularly polarized tightly coupled crossed dipole array (CP-TCCDA) with wide overlapped impedance bandwidth and axial ratio (AR) bandwidth. A tightly coupled crossed dipole unit cell is investigated and the comparison with an isolated crossed dipole of the same size indicates that the VSWR<3 bandwidth is increased from 3:1 to 7.1:1 while the 3-dB AR bandwidth is increased from 1.3:1 to 2.1:1. Analysis is given to explain the principles of AR bandwidth improvement and is verified by the comparison of radiated E-fields between a CP-TCCDA and a conventional crossed dipole array. To verify the design concept, a 4 × 4 CP-TCCDA with feeding network is fabricated and measured. The measured results confirm that the proposed array achieves VSWR<3 bandwidth from 2.06GHz to 6.46 GHz (3.14:1) and 3-dB AR bandwidth from 2.35GHz to 5.6GHz (2.38:1), which are much wider than the bandwidth of an isolated element and a conventional array using the same element.**

Index Terms—Crossed dipole, circular polarization, tightly coupled array, wideband array.

I. Introduction

With rapid development of various wireless communication systems, wideband antennas and arrays are becoming increasingly important to multifunctional systems, high-data-rate communication links, high-resolution radar and tracking systems, software radios and electronic warfare applications [1]. To design wideband arrays, wideband antenna elements, such as the Vivaldi antenna and "bunny-ear" antenna are normally used. However, the considerable height limits their applications to some extent.

Instead of using elements with inherent broad bandwidth to build a wideband array, Munk used capacitively coupled short dipoles to design a wideband array which achieved 4.5:1 impedance bandwidth [2]. The idea was to alleviate inductive loading introduced by the ground plane using capacitive coupling among neighboring elements. Due to the closely spaced dipole configuration, these elements are tightly coupled and the electric current along each dipole is almost constant, which is distinct from the electric current on a single dipole where a sinusoidal magnitude distribution with nulls at the termination exists [3]. This kind of dipole array emulated Wheeler's electric current sheet which can support radiation at much lower frequencies than the element's self-resonant frequency [4].

Two different types of arrays were proposed to realize Wheeler's current sheet and both obtained wide bandwidth. The first one was the "connected arrays" which interconnected array elements to achieve relatively constant electric current across the array aperture and large array bandwidth [5, 6]. Another type was the "tightly coupled array" which utilized closely spaced dipoles, where the strong mutual coupling among the dipole elements facilitated the improvement of array bandwidth [7, 8].

Although the aforementioned arrays achieved several octave bandwidths, they were all linearly polarized or dual linearly polarized and only the impedance bandwidth was considered. For applications such as the high-data-rate satellite communications, wideband circularly polarized (CP) antennas and arrays are preferred [9]. However, there are few reported CP array designs based on the concept of connected array or tightly-coupled array. A dual-CP spiral array in which neighboring spirals of orthogonal polarizations were connected achieved 1.8 times AR bandwidth than the single spiral [10]. The AR bandwidth enhancement in this design was mainly due to the doubling of the electric travelling-wave current path. By connecting more spirals in a ring-array structure, the AR bandwidth was further improved [11]. A spiral array within which the arms of the spiral elements were interwoven achieved a 10:1 bandwidth [12]. However, within this 10:1 frequency range, the average difference between the RHCP and LHCP gains were only 7 dB indicating that the AR performance of the array was not good (average AR within the operating band was around 8.4 dB).

Recently, a crossed dipole structure which incorporated 90^{o} phase shift line between the orthogonally placed dipoles were presented [13]. Because of the incorporated 90^{o} phase shift line, the crossed dipole antenna was able to be fed by a coaxial connector directly without any baluns and still achieved good CP performance. Based on the CP crossed dipole, a CP tightly coupled array is developed in this paper. The proposed design utilizes two orthogonally polarized electric fields but is different to the dual-polarized tightly coupled array [14] where the dipoles of different polarization were fed offset by $\lambda/4$. In the proposed design, the orthogonally polarized dipoles are fed concentrically with an inherent 90^{o} phase shift. By decreasing the element space and choosing appropriate overlapped structure between adjacent elements, it is shown that not only the impedance bandwidth but also the AR bandwidth of the array is greatly improved compared with the single isolated element. To verify the concept, a 4×4 array is prototyped and the measurement results confirm that the proposed CP tightly coupled array achieves a 3.14:1 VSWR<3 bandwidth and a 2.38:1 3-dB AR bandwidth, which shows much wider bandwidth than the conventional crossed dipole array using the same element.

II. Tightly Coupled Crossed Dipole Unit Cell

A. Unit Cell Configuration

To predict the performance of an infinite array, the unit cell under periodic boundary gives a good approximation. The configuration of

Manuscript received on February 23, 2017.

L. Zhang and Y. He are with Shenzhen Key Laboratory of Antennas and Propagation, College of Information Engineering, Shenzhen University, Shenzhen 518060, China. (email: longzhang717@163.com).

S. Gao, Q. Luo and W. Li are with the School of Engineering and Digital Arts, University of Kent, Canterbury CT2 7NT, UK.(email: s.gao@kent.ac.uk).

Q. Li is with the School of Electronic Information and Communications, Huazhong University of Science and Technology, Wuhan 430074, China.

the tightly coupled dipole unit cell is shown in Fig. 1.

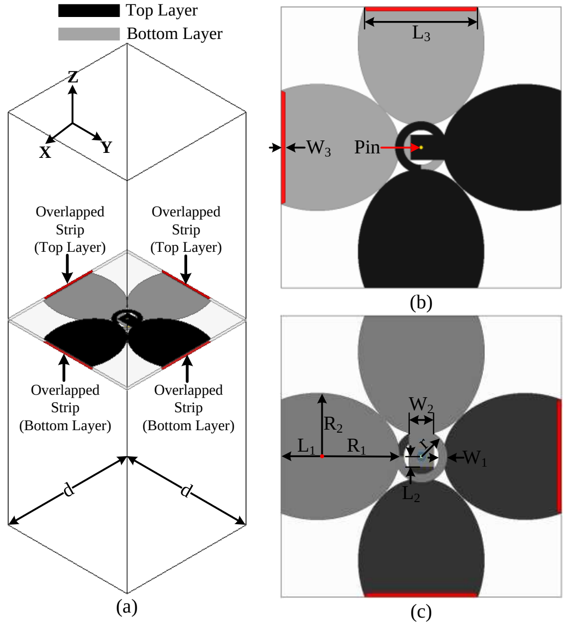

Fig. 1. Geometry of the unit cell: (a) 3D view, (b) top view, (c) bottom view.

The proposed element is printed on both sides of a 0.813mm thick Rogers RO4003C substrate. As shown, two neighboring cutting-off elliptical arms are connected by a ¾ ring shaped phase shift line with outer radius r and line width W_1. This ¾ ring shaped line provides 90º phase shift between the neighboring arms, which makes the crossed dipoles radiate CP wave. Besides, the top-layer arms are connected to the inner pin of a coaxial cable while the bottom-layer arms are connected to the outer conductor and no ground plane is used. To imitate an infinite tightly coupled array, the proposed element is placed in periodic boundaries with a unit cell size of d × d and four overlapped strips are utilized to provide strong capacitive coupling between adjacent elements along both x- and y- directions. The detailed geometry dimensions of the unit cell are given in Table I.

TABLE I
UNIT CELL DIMENSIONS (mm)

d	L_1	L_2	L_3	W_1	W_2	W_3	R_1	R_2	r
40	5.2	1.5	16.1	1.2	3.5	0.6	11.7	9	3.7

B. Comparison with the Isolated Crossed Dipole

An isolated crossed dipole with the same size as the element used in the infinite tightly coupled crossed dipole array is also simulated for a comparison. Fig. 2 shows the comparison of these two elements in terms of VSWR and AR.

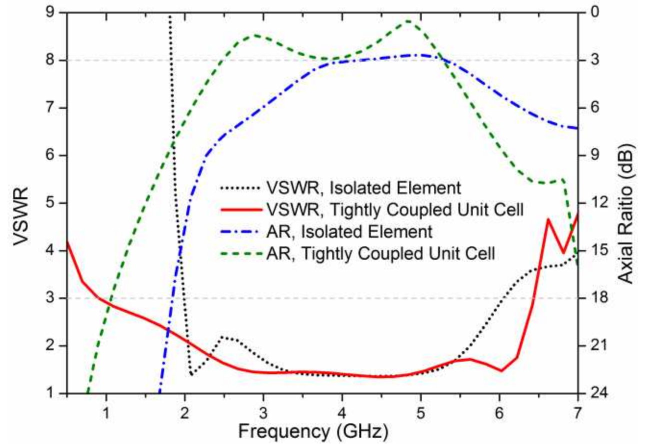

Fig. 2. Comparison of the VSWR and AR between the isolated element and the tightly coupled unit cell.

As shown in Fig. 2, the simulated VSWR<3 bandwidth of the isolated element is 2-6 GHz (3:1) while the corresponding bandwidth of the tightly coupled unit cell is 0.9-6.4 GHz (7.1:1). Greatly improved impedance bandwidth at lower frequency is observed, similar to those linearly polarized tightly coupled unit cell [7, 8]. Furthermore, it is shown that the AR bandwidth improves from 4-5.3 GHz (1.325:1) to 2.4-5.3GHz (2.21:1) by the tightly coupled unit cell.

III. ANALYSIS AND DESIGN OF THE 4×4 CP-TCCDA

A. Analysis of the Bandwidth Enhancement

As demonstrated in Section II, the bandwidth of a CP crossed dipole can be improved through using a tightly coupled array. The impedance bandwidth enhancement can be explained by the lengthening of the electric current or equivalent increase of the antenna's electrical length, which decreases the array's lower limit working frequency range while the upper limit of the working frequency range is mainly controlled by the element and thus varies slightly.

The phase difference between the two orthogonally placed dipoles is mainly introduced by the ¾ ring shaped phase shift line and its length is calculated by

$$l_{phase\ shift} = 2\pi \times (r - W_1/2) \times 3/4 \tag{1}$$

where r, W_1 and W_2 are parameters shown in Table I. The calculated physical length of the ¾ ring shaped phase shift line is around 14.6mm which equals to a quarter of the guided wavelength at 3.08GHz.

Considering an elliptically polarized wave with its AR calculated by [15]

$$AR = \frac{E_{major\ axis}}{E_{minor\ axis}} = \frac{OA}{OB}\ , 1 \le AR \le \infty \tag{2}$$

where

$$OA = \left\{\frac{1}{2}\left[{E_x}^2 + {E_y}^2 + \left({E_x}^4 + {E_y}^4 + 2{E_x}^2{E_y}^2\cos 2\delta\right)^{\frac{1}{2}}\right]\right\}^{\frac{1}{2}} \tag{3}$$

$$OB = \left\{\frac{1}{2}\left[{E_x}^2 + {E_y}^2 - \left({E_x}^4 + {E_y}^4 + 2{E_x}^2{E_y}^2\cos 2\delta\right)^{\frac{1}{2}}\right]\right\}^{\frac{1}{2}} \tag{4}$$

Since the infinite CP-TCCDA has enough electrical lengths along x- and y- direction at 2.4GHz, it is reasonable to deem the magnitude of the radiated E-fields along x- and y- direction is close to each other at 2.4GHz, i.e.,

$$E_x \approx E_y \tag{5}$$

As the phase difference introduced by the ¾ ring shaped phase shift line is around 90º at 3.08GHz, the phase difference between E_x and E_y at 2.4GHz is

$$\delta = \frac{\pi}{2} \times \frac{2.4}{3.08} = 0.39\,\pi \tag{6}$$

Substituting (5) and (6) into (2)-(4) and calculate the AR at 2.4 GHz yields a result of 1.425 (3.07 dB), which is very close to the simulation result shown in Fig. 2. From the above analysis and calculation result, we obtain the following conclusions:

1) The AR bandwidth enhancement of the CP-TCCDA is mainly attributed to the strong mutual coupling which enables the array to radiate more evenly along x- and y- directions at much lower frequencies. Although the VSWR of the single isolated element at 2.4GHz is around 2, the smaller electrical length than the CP-TCCDA may result in deterioration of the magnitude balance and possible phase difference variations between x- and y- directions.

2) Although the impedance bandwidth of CP-TCCDA can reach a lower limit of 0.9GHz, the AR bandwidth cannot approach this limit. Considering that the phase difference between $\overrightarrow{E_x}$ and $\overrightarrow{E_y}$ is determined by the electrical length of the ¾ ring shaped phase shift line, the phase difference between the two orthogonal E-fields at 0.9GHz is around 26.3º. Assuming $E_x = E_y$ and the AR at 0.9GHz is calculated to be 12.6 dB. Notice that at this frequency, actually the magnitudes of the E-fields along x- and y- direction may have certain differences and thus the AR should be higher than 12.6 dB. Thus, the AR bandwidth limitation of the proposed array is mainly attributed to the variation of the phase difference between the two orthogonal electric fields when frequency changes.

B. 4×4 CP-TCCDA and 4×4 Conventional Crossed Dipole Array

To verify the above analysis and the presented concept, a 4×4 CP-TCCDA is designed. The configuration of the 4×4 CP-TCCDA is shown in Fig. 3 while the magnified picture demonstrates the overlapped area in detail. As shown, the width of the overlapped part is 1.2mm which is twice the width of the overlapped strip in the unit cell. The element space is 40mm which is the same as the unit cell size given in Fig. 1. Furthermore, to make a direct comparison with a conventional array, a 4×4 conventional array using the isolated element is also designed. The element space of the 4×4 conventional array is chosen to be half free-space wavelength at 2.4GHz (62.5mm). With this element space, the array has much smaller coupling than the CP-TCCDA.

Fig. 4 shows simulated E-fields of the two arrays at 2.4GHz in a plane parallel to the array aperture at the height of 55 mm. The magnitudes of the two fields are normalized to the same scale for better comparison. As the E-fields along broadside direction relate to the array's AR bandwidth, the E-fields at the center area of each graph are of major interest. As shown, both the 4×4 CP-TCCDA and the 4×4 conventional coupled array have a rotated E-fields distribution at different time slot. However, the magnitudes of the E-fields of the 4×4 conventional coupled array are quite different for the radiated E-fields along x- and y-direction (E_x and E_y). On the contrary, the radiated E-fields of the 4×4 CP-TCCDA along x- and y- direction are nearly the same in the center area, which verifies the assumption of equation (5). As the phase difference between $\overrightarrow{E_x}$ and $\overrightarrow{E_y}$ of the two arrays are both determined by the ¾ ring shaped phase shift line, the phase differences between $\overrightarrow{E_x}$ and $\overrightarrow{E_y}$ of the two arrays are the same at 2.4GHz. However, the unequal (unbalanced) magnitudes of $\overrightarrow{E_x}$ and $\overrightarrow{E_y}$ of the 4×4 conventional coupled array result in a larger AR compared with the 4×4 CP-TCCDA, according to equations (2)-(4).

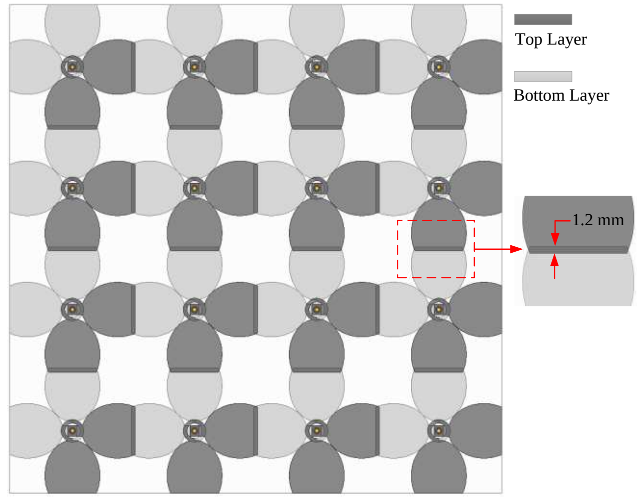

Fig. 3. Configuration of the 4×4 CP-TCCDA.

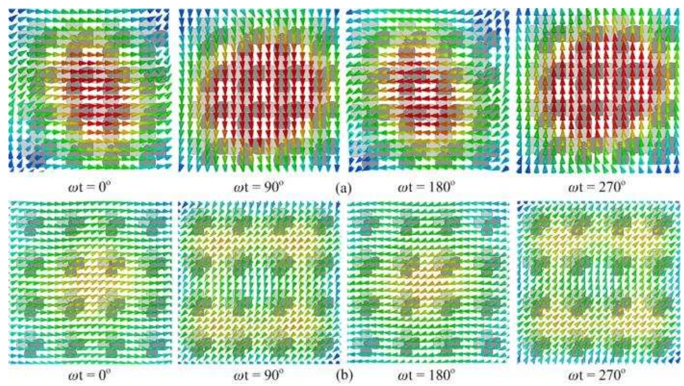

Fig. 4. Comparison of the E-fields at 2.4GHz: (a) 4×4 CP-TCCDA, (b) 4×4 conventional array.

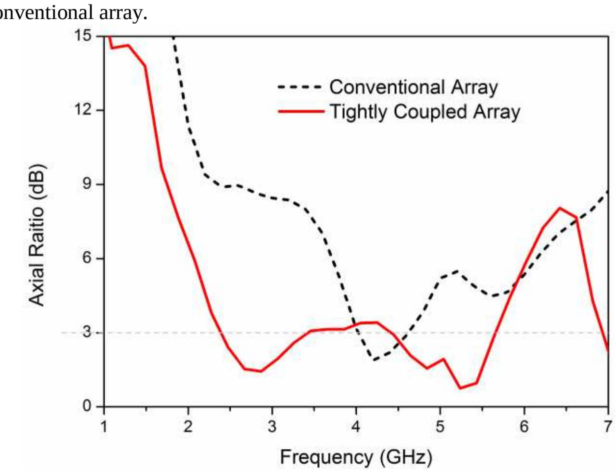

Fig. 5. Comparison of the AR between the 4×4 CP-TCCDA and 4×4 conventional crossed dipole array.

The comparison of the AR between the 4×4 CP-TCCDA and 4×4 conventional crossed dipole array is shown in Fig. 5. As shown, the 3-dB AR bandwidth of the 4×4 CP-TCCDA is much wider than the conventional crossed dipole array. Moreover, the simulated AR performance of the 4×4 CP-TCCDA is close to the simulated AR of the infinite CP-TCCDA due to the fact that the 4×4 CP-TCCDA is able to maintain balanced magnitudes of $\overrightarrow{E_x}$ and $\overrightarrow{E_y}$ at low frequencies.

C. 1:16 Wilkinson Power Divider Network

To feed the 4×4 CP-TCCDA, a 1:16 Wilkinson power divider network is designed and shown in Fig. 6. Since the CP-TCCDA achieves a 3dB AR bandwidth from 2.4 to 5.3GHz (2.21:1), the bandwidth of the power divider network is designed to cover this frequency range.

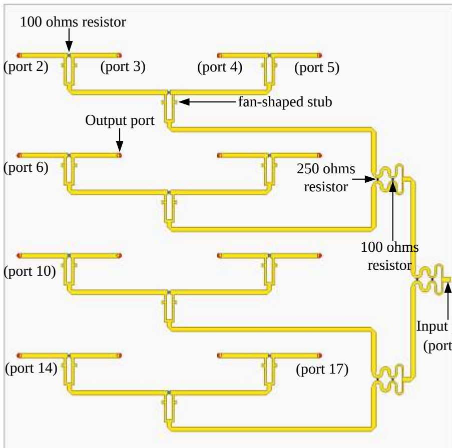

Fig. 6. 1:16 Wilkinson power divider network.

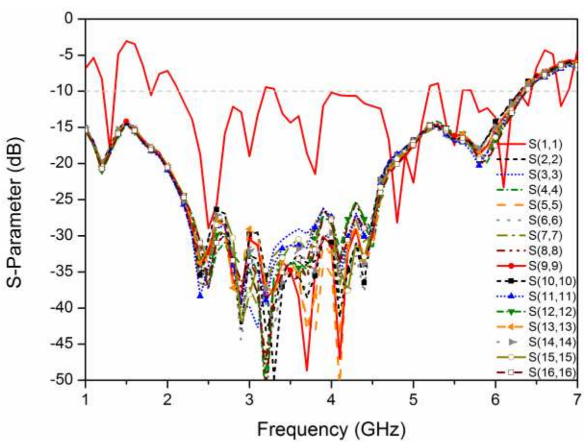

Fig. 7. Simulated reflection coefficients of the power divider network.

The simulated reflection coefficients of all ports are shown in Fig. 7. As shown, the input port (port 1) achieves -10dB reflection coefficient from 2.1 to 6.3GHz while all other ports' reflection coefficients are smaller than -10dB from 1 to 6.3GHz. From the simulation, the input power is divided equally into the 16 output ports and the insertion loss is around 1-2 dB from 2 to 6.3GHz, which meets the bandwidth coverage requirement.

IV. Results and Discussion

To verify the design concept and analysis, a 4×4 CP-TCCDA with feeding network is prototyped and measured.

A. Prototype

The fabricated 4×4 CP-TCCDA is shown in Fig. 8. As shown, the array is placed above an Eccosorb AN-77 absorber which helps achieve directional radiation and maintain good bandwidth performance. The thickness of the absorber is 5.7 cm while the height of the array is 12 cm. There are 16 coaxial cables with outer conductor soldered to the bottom-layer arms and inner pin soldered to the top-layer arms of the proposed array, which is demonstrated by Fig. 8 (d). These cables are then connected to the 1:16 power divider network which is shown in Fig. 9. For this array configuration, the array height is mainly determined by the thickness of the absorber and assembling requirements.

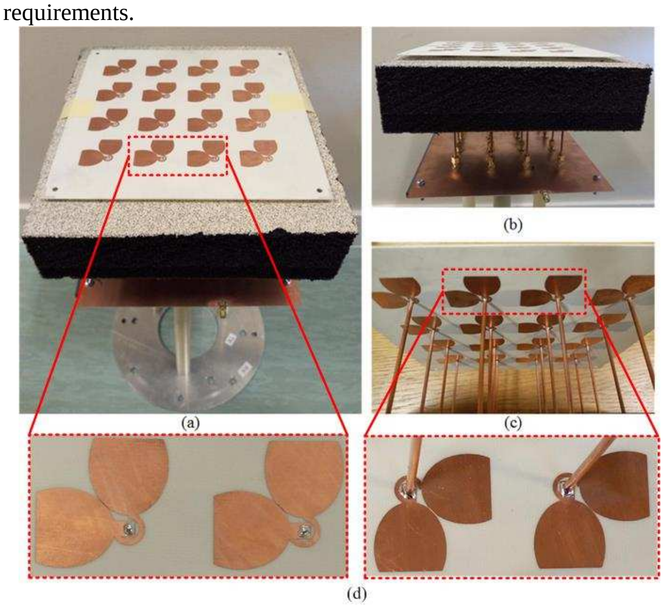

Fig. 8. 4×4 CP-TCCDA prototype: (a) front view, (b) side view, (c) bottom view, (d) feeding details.

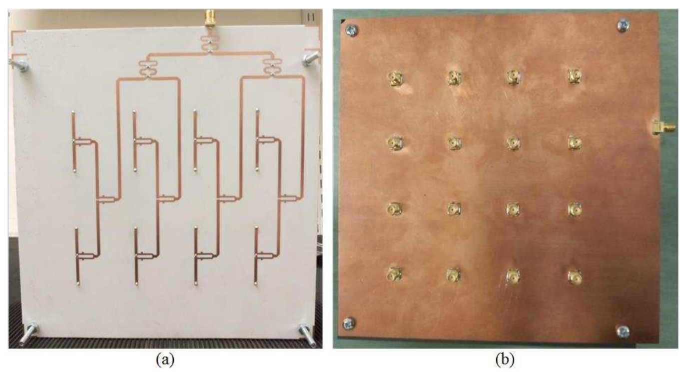

Fig. 9. 1:16 Wilkinson power divider network prototype: (a) top view, (b) bottom view (ground plane with 16 coaxial connectors).

B. VSWR and AR

The simulated and measured VSWR of the proposed 4×4 CP-TCCDA is shown in Fig. 10. It is worth pointing out that the simulated curve indicates the active VSWR of one center element, which is better than the VSWR of peripheral elements. As the measured result combines the VSWR of all 16 ports, the measured result is worse than the simulated result. As shown, the measured VSWR<3 bandwidth is from 2.06GHz to 6.46 GHz (3.14:1). The measured VSWR is smaller than 2.5 within most of the bandwidth. Compared with the simulated VSWR, ripples are constantly occurred, which is caused by the multiple reflections from the power divider network, as shown in Fig. 7.

It is noted that no obvious common mode resonance is observed in the results. One reason may be the utilization of the absorber which helps suppress the net vertically polarized currents undergoing strong resonances. When the array is scanned, the VSWR of the array will degrade due to the unbalanced push-pull currents and the common mode resonances [16]. Generally, the array works well when it scans to broadside and small angles but will undergo performance degradation to some extent when it scans to large angles.

Fig. 10 also shows the simulated and measured AR bandwidth. The measured result indicates that the proposed 4×4 CP-TCCDA achieves 3-dB AR bandwidth from 2.35GHz to 5.6GHz (2.38:1).

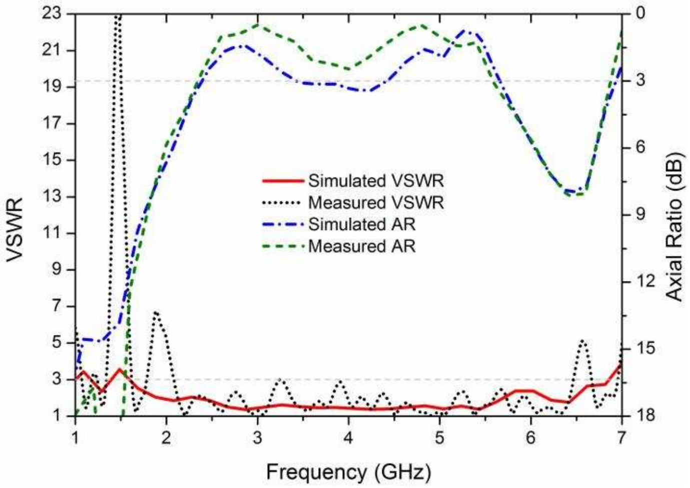

Fig. 10. Simulated and measured VSWR.

C. Radiation Patterns

The simulated and measured radiation patterns are shown in Fig. 11. Good agreements between the simulation and measurement results are observed. It is also shown that the proposed array achieves undistorted beams and lower than -15dB cross-pol over a 2.1:1 frequency range.

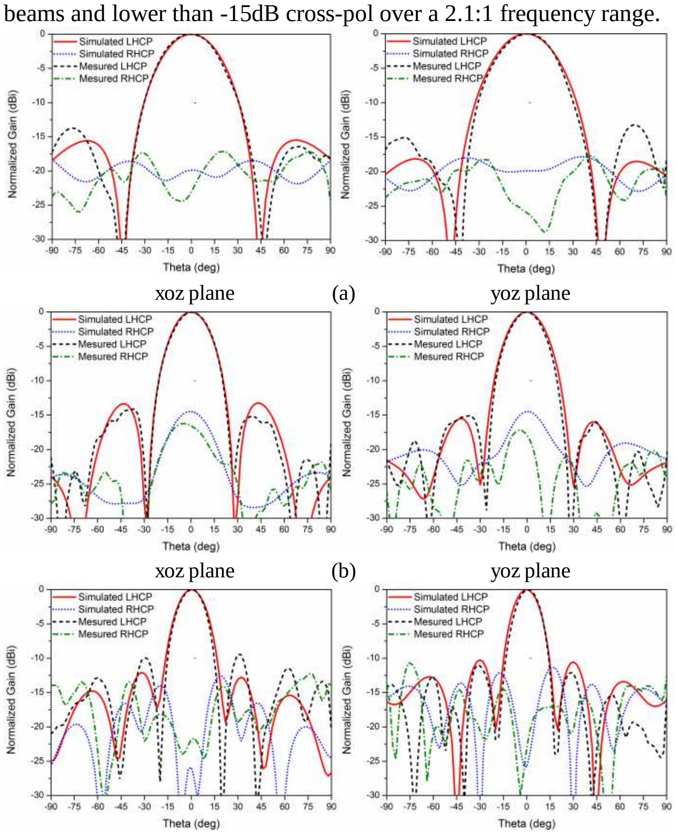

Fig. 11. Simulated and measured radiation patterns at: (a) 2.6GHz, (b) 4GHz, (c) 5.4GHz

D. Gain

The simulated and measured gain is shown in Fig. 12. The insertion loss of the feeding network is compensated when calculating the measured gain. As shown, the antenna gain increases as frequency increases within the working bandwidth, which is similar to those reported linearly polarized tightly coupled arrays. The reduction of the array gain around 5.5 GHz may be attributed to the finite size of the antenna array [17]. Moreover, an additional curve which indicates the gain of an ideal array with the same aperture size and 100% aperture efficiency is included in Fig. 12 for reference. Due to the presence of the absorber, the array gain is around 4 dB smaller than the gain of the ideal array within the operating band.

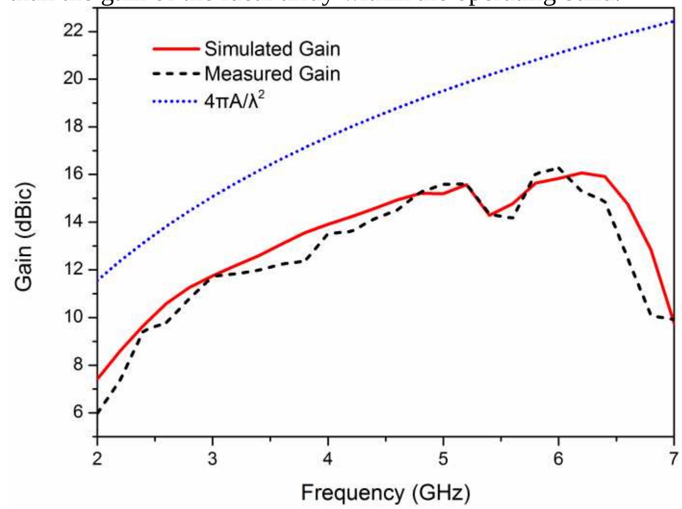

Fig. 12. Simulated and measured gain.

V. CONCLUSION

A wideband circularly polarized tightly coupled crossed dipole array which uses the strong coupling between adjacent elements to improve the AR bandwidth of the array is proposed in this communication. Analysis is given to interpret the AR bandwidth improvement mechanism and it is found that the balanced electric fields along x- and y- directions over a wide frequency range lead to the enhancement of AR performance. A 4×4 CP-TCCDA with feeding network is fabricated and the measured results validate the design concept. Owing to the concurrent wide impedance bandwidth and wide AR bandwidth, the proposed CP-TCCDA is promising for applications in various wireless systems which need large bandwidth.

REFERENCES

[1] J. P. Doane, K. Sertel, and J. L. Volakis, "A wideband, wide scanning tightly coupled dipole array with integrated balun (TCDA-IB)," IEEE Trans. Antennas Propag., vol. 61, pp. 4538-4548, 2013.

[2] B. A. Munk, Finite antenna arrays and FSS: John Wiley & Sons, 2003.

[3] E. Yetisir, N. Ghalichechian, and J. L. Volakis, "Ultrawideband Array With 70° Scanning Using FSS Superstrate," IEEE Trans. Antennas Propag., vol. 64, pp. 4256-4265, 2016.

[4] H. Wheeler, "Simple relations derived fom a phased-array antenna made of an infinite current sheet," IEEE Trans. Antennas Propag., vol. 13, pp. 506-514, 1965.

[5] D. Cavallo and A. Neto, "A connected array of slots supporting broadband leaky waves," IEEE Trans. Antennas Propag., vol. 61, pp. 1986-1994, 2013.

[6] R. J. Bolt, D. Cavallo, G. Gerini, D. Deurloo, et al., "Characterization of a Dual-Polarized Connected-Dipole Array for Ku-Band Mobile Terminals," IEEE Trans. Antennas Propag., vol. 64, pp. 591-598, 2016.

[7] J. A. Kasemodel, C.-C. Chen, and J. L. Volakis, "Wideband planar array with integrated feed and matching network for wide-angle scanning," IEEE Trans. Antennas Propag., vol. 61, pp. 4528-4537, 2013.

[8] M. H. Novak and J. L. Volakis, "Ultrawideband antennas for multiband satellite communications at UHF – Ku frequencies," IEEE Trans. Antennas Propag., vol. 63, pp. 1334-1341, 2015.

[9] S. Gao, Q. Luo, and F. Zhu, Circularly polarized antennas: John Wiley & Sons, 2013.

[10] R. Guinvarc'h and R. L. Haupt, "Connecting spirals for wideband dual polarization phased array," IEEE Trans. Antennas Propag., vol. 59, pp. 4534-4541, 2011.
[11] I. D. H. Sáenz, R. Guinvarc'h, R. L. Haupt, and K. Louertani, "A 6: 1 Bandwidth, Low-Profile, Dual-Polarized Ring Array of Spiral Antennas With Connecting Arms," IEEE Trans. Antennas Propag., vol. 64, pp. 752-756, 2016.
[12] I. Tzanidis, K. Sertel, and J. L. Volakis, "Interwoven spiral array (ISPA) with a 10: 1 bandwidth on a ground plane," IEEE Antennas Wireless Propag. Lett., vol. 10, pp. 115-118, 2011.
[13] J.-W. Baik, T.-H. Lee, S. Pyo, S.-M. Han, et al., "Broadband circularly polarized crossed dipole with parasitic loop resonators and its arrays," IEEE Trans. Antennas Propag., vol. 59, pp. 80-88, 2011.
[14] D. K. Papantonis and J. L. Volakis, "Dual-polarized tightly coupled array with substrate loading," IEEE Antennas and Wireless Propagation Letters, vol. 15, pp. 325-328, 2016.
[15] C. A. Balanis, Antenna theory: analysis and design: John Wiley & Sons, 2016.
[16] S. S. Holland and M. N. Vouvakis, "The planar ultrawideband modular antenna (PUMA) array," IEEE Trans. Antennas Propag., vol. 60, pp. 130-140, 2012.
[17] S. S. Holland, D. H. Schaubert, and M. N. Vouvakis, "A 7–21 GHz dual-polarized planar ultrawideband modular antenna (PUMA) array," IEEE Trans. Antennas Propag., vol. 60, pp. 4589-4600, 2012.